Materials Letters 277 (2020) 128384

Contents lists available at ScienceDirect

Materials Letters

journal homepage: www.elsevier.com/locate/mlblue

3D morphology and growth mechanism of cubic α-Al(FeMnCr)Si intermetallic in an Al-Si cast alloy

Dongtao Wang [a,b], Xiaozu Zhang [a,b], Hiromi Nagaumi [a,b,*], Xinzhong Li [a,b], Haitao Zhang [a,c]

[a] High-Performance Metal Structural Materials Research Institute, Soochow University, Suzhou, Jiangsu 215021, China
[b] Shagang School of Iron and Steel, Soochow University, Suzhou, Jiangsu 215021, China
[c] Key Laboratory of Electromagnetic Processing of Materials, Ministry of Education, Northeastern University, Shenyang, Liaoning 110819, China

ARTICLE INFO

Article history:
Received 2 May 2020
Received in revised form 9 July 2020
Accepted 20 July 2020
Available online 23 July 2020

Keywords:
Crystal growth
Solidification
Intermetallic
Al-Si alloy

ABSTRACT

3-D morphology and growth mechanism of α-Al(FeMnCr)Si crystal were investigated by extracting Fe-containing intermetallics in slow-cooled Al-7Si-1Fe-1.5Mn-0.5Cr (wt%) alloy. It is found that cube is the dominated growth morphology of α-Al(FeMnCr)Si intermetallic crystal. It is covered by six {100} faces and shows preferential growth in eight points of the cube. Series of transition morphologies are also observed which corresponds to different growth stages of the crystal before forming a final cube. After a careful interconnection of these morphologies and further combination of crystal growth theory, the growth mechanism and the transition evolution of the cubic α-Al(FeMnCr)Si intermetallic crystal are put forward. This is reasonably identical with the experimental results.

1. Introduction

Fe is one of the main impurities in aluminum alloys, which tends to form Fe-containing intermetallics and potentially induce brittleness of the alloys [1–4]. Much research [1,5,6] has focused on the crystal growth morphologies of typical β-AlFeSi and α-Al(FeMn)Si in order to understand their growth mechanism and thus seek methods to eliminate the negative effects of the Fe-containing intermetallics. Various morphology has been observed, typically acicular and plate-like shapes [5] for β-AlFeSi and dodecahedron [6] for α-Al(FeMn)Si in Al-Si cast alloys. Terzi et al. [5] suggested that the β-AlFeSi shows non-crystallographically interconnected plates, which grow rapidly in the lateral direction and with much slower rates for thickening. Gao et al. [6] proposed that the α-Al(FeMn)Si exhibits rhombic dodecahedron which are covered by twelve {110} faces due to their lower growth rates. The chemical difference between β-AlFeSi and α-Al(FeMn)Si induces the large difference in their growth morphology and pattern.

In Al-Si cast alloys, Mn and Cr are added to strengthen the mechanical properties, but high Fe level (>0.3 wt%) in Al-Si-Mn-Cr alloy results in the formation of the quinary α-Al(FeMnCr)Si phase [7–10]. This intermetallic compound precipitates from liquid at a higher temperature than that for β-AlFeSi and α-Al(FeMn)Si due to the introduction of the refractory Cr. Correspondingly, the intermetallic crystal tends to be coarse in size and exhibit a wide range of morphologies due to its inherent faceted growth pattern with strong anisotropy. Results by in-situ examination of X-radiographic [11] show complex growth morphologies of α-Al(FeMnCr)Si during solidification at different cooling rates, typically rhombic dodecahedron, elongated rod, star-shape and dendrite.

Because the coarse Fe-containing intermetallics are detrimental to mechanical properties of Al-Si alloy, it is necessary to separate them from melt, decrease the Fe level and thus reduce its detrimental effect to the alloy. Physical separation process, such as gravity sedimentation and electromagnetic separation, is commonly used to separate Fe-containing intermetallic from Al melt [12–14]. The morphology of the intermetallic crystal is important to the separation efficiency [13]. Typically, the intermetallic with regular morphology shows less moving resistance in melt. Chen et al. suggested that electromagnetic separation efficiency was increased by 20% when the morphology of Fe-containing intermetallic transformed from acicular to bulk shapes after Mn addition [14]. However, the Fe-containing intermetallics with complex composition shows complicated growth patterns and morphologies.

Therefore, a further research on 3D morphology and the growth mechanism of this intermetallic compound is still needed in order to control and optimize its morphology and thus develop better physical means to efficiently remove it from the melt, eliminating the negative effect of high Fe level. In this work, we focus on the crystal growth of α-Al(FeMnCr)Si during solidification at a low

* Corresponding author.
E-mail address: zhanghai888jp@suda.edu.cn (H. Nagaumi).

https://doi.org/10.1016/j.matlet.2020.128384
0167-577X/

cooling rate. The resulted growth morphology is studied for clarifying the potential growth behavior and mechanism.

2. Experimental procedures

Al-7Si-1Fe-1.5Mn-0.5Cr (wt%) alloy was prepared by medium frequency induction melting. Al-20 wt%Si master alloy was first melted at 780 °C, and then Al-10 wt%Fe, Al-20 wt%Mn and Al-10 wt%Cr master alloy were added in the melt. After holding at 810 °C for 30 min, the alloy melt was poured into a cylindrical graphite mold (diameter 120 mm, height 100 mm), preheating to 720 °C. As-cast samples were taken from the 1/2 height location of mold. The measured cooling rate of the melt is about 1.5 K/s. Microstructural analysis for the samples was carried out using scanning electron microscopy (SEM) equipped with X-ray energy dispersive spectroscopy (EDS). The Al matrix was dissolved by electrolyzing specimen in 2% NaCl solution, in order to extract the α-Al(FeMnCr)Si intermetallics for 3D morphology analysis. The cathode of lead bulk was used. The voltage of electrolytic process was controlled in the range of 10 ~ 15 V, and the current of electrolytic process was 2 ~ 3 A. The time of electrolytic extraction was about 30 ~ 50 min. Additionally, thermal history during solidification of the alloy were characterized using a NETZSCH 420 differential scanning calorimeter (DSC). The solidification sequence of the alloy was calculated by JMatPro thermodynamic software.

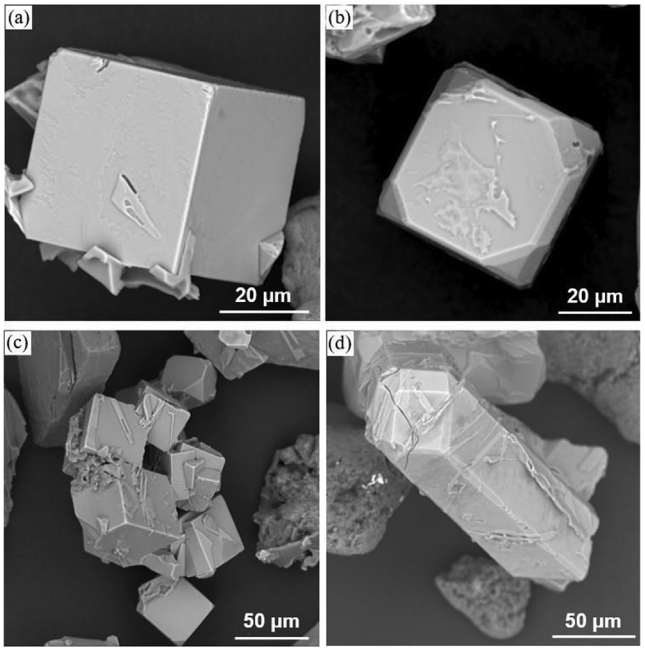

Fig. 2. Typical 3D morphologies of α-Al(FeMnCr)Si crystals: (a) perfect cube; (b) truncated cube; (c) agglomeration of cube; (d) elongated hexahedron.

3. Results and discussion

Fig. 1 shows the microstructure and solidification sequence of Al-7Si-1Fe-1.5Mn-0.5Cr (wt%) alloy. Fe-containing intermetallics, α-Al and Al-Si eutectic are found in Fig. 1(a). A faceted growth of the Fe-containing intermetallics can be observed clearly, which exhibits polygonal and irregular shapes, as shown in Fig. 1(b). The chemical composition (at%) of the Fe-containing intermetallics is determined by EDS in Fig. 1(c), typically Al 63.39%, Mn 18.05%, Si 8.89%, Fe 6.73% and Cr 2.94%. The calculated solidification sequence for the alloy shows that the α-Al(FeMnCr)Si is the primary phase during solidification with a precipitation temperature at about 710 °C, as shown in Fig. 1(d). This temperature is nearly identical with the measured result by DSC in Fig. 1(e).

Fig. 2 shows the typical 3D morphologies of α-Al(FeMnCr)Si intermetallics. A perfect cubic crystal is observed in Fig. 2(a), and the truncated cube α-Al(FeMnCr)Si can be observed in Fig. 2(b). In addition, the agglomeration of cubic α-Al(FeMnCr)Si intermetallics in Fig. 2(c) and an elongated hexahedron in Fig. 2(d)

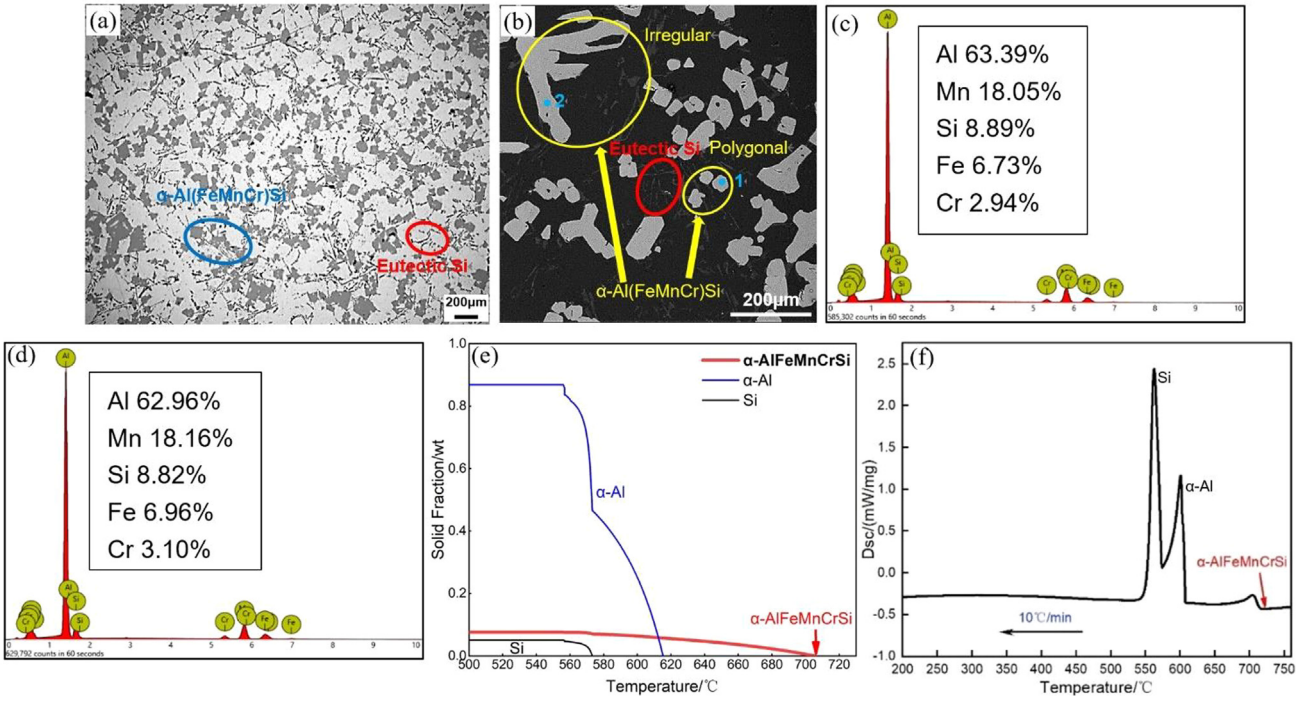

Fig. 1. (a) OM micrograph of the alloy; (b) SEM image showing 2D morphology of α-Al(FeMnCr)Si; (c) EDS result of α-Al(FeMnCr)Si at position 1; (d) EDS result of α-Al(FeMnCr)Si at position 2; (e) calculated solidification path of the alloy; (f) DSC pattern of the alloy.

are also found. Actually, the morphologies in Fig. 2(b), (c) and (d) can be regarded as the derivative morphologies of cube α-Al(FeMnCr)Si. Their difference is mainly attributed to the difference in growth conditions for each crystallographic plane, related to the chemical and thermal aspects. Thus, it can be deduced that one single crystal of the α-Al(FeMnCr)Si in homogeneous liquid tends to form perfect cube during nearly equilibrium solidification.

The result in Fig. 2 clearly shows that the cubic crystal is the dominated growth morphology of the α-Al(FeMnCr)Si in the present alloy. In order to further observe the transitional morphologies, the alloy melt was holding at 680 °C for different times (5–40 min) after being poured into a preheated cylindrical graphite mold and then the melt was slowly cooled at ~1.5 K/s. After short holding times (5–15 min), some other morphologies of the intermetallic crystal are also observed in the alloy, as shown in Fig. 3. They correspond to different growth stages of the crystal since the nucleation and growth of crystals occur alternately during the bulk solidification process. A trace of the crystal growth can be deduced after a careful comparison and interconnection of these morphologies. Fig. 3 shows the corresponding morphology evolution at different growth stages. In initial stage of growth, the growth tip in Fig. 3(a) preferentially appears and acts as the preferential growth parts in Fig. 3(b). With the further growth of the crystal, defects of hollow and edge appear in {100} faces of the cubic crystal in Fig. 3(c). In this growth stage, the preferential growth parts in Fig. 3(b) have interconnected and defects of hollow and edge do not fill completely. This clearly shows the growth anisotropy of this intermetallic crystal. In Fig. 3(d), the edge defects have been filled gradually and the hollow defects still retain. Normally, the edge of crystal is easier to growth completely and the center of crystal face is more difficult to fill solute atoms resulting in the hollow defect [15]. Fig. 3(e) shows the crystal with only hollow defects. In this stage, the edge defects have been filled completely. Fig. 3(f) shows the complete cube α-Al(FeMnCr)Si when the hollows in the face centers were finally filled. Meanwhile, the truncated cube α-Al(FeMnCr)Si can be observed in Fig. 3(g). It suggests that the growth rates of {1 1 0} faces decrease in some cubic α-Al(FeMnCr)Si crystal and the {1 1 0} faces retain finally.

Fig. 4 shows the predicted growth process of the cubic α-Al(FeMnCr)Si crystal based on the observation in Figs. 2 and 3. During the initial solidification, the nucleation of the crystal preferentially happens at the position with high concentrations of Fe, Si, Mn, Cr in the melt. It tends to be sphere according to minimum

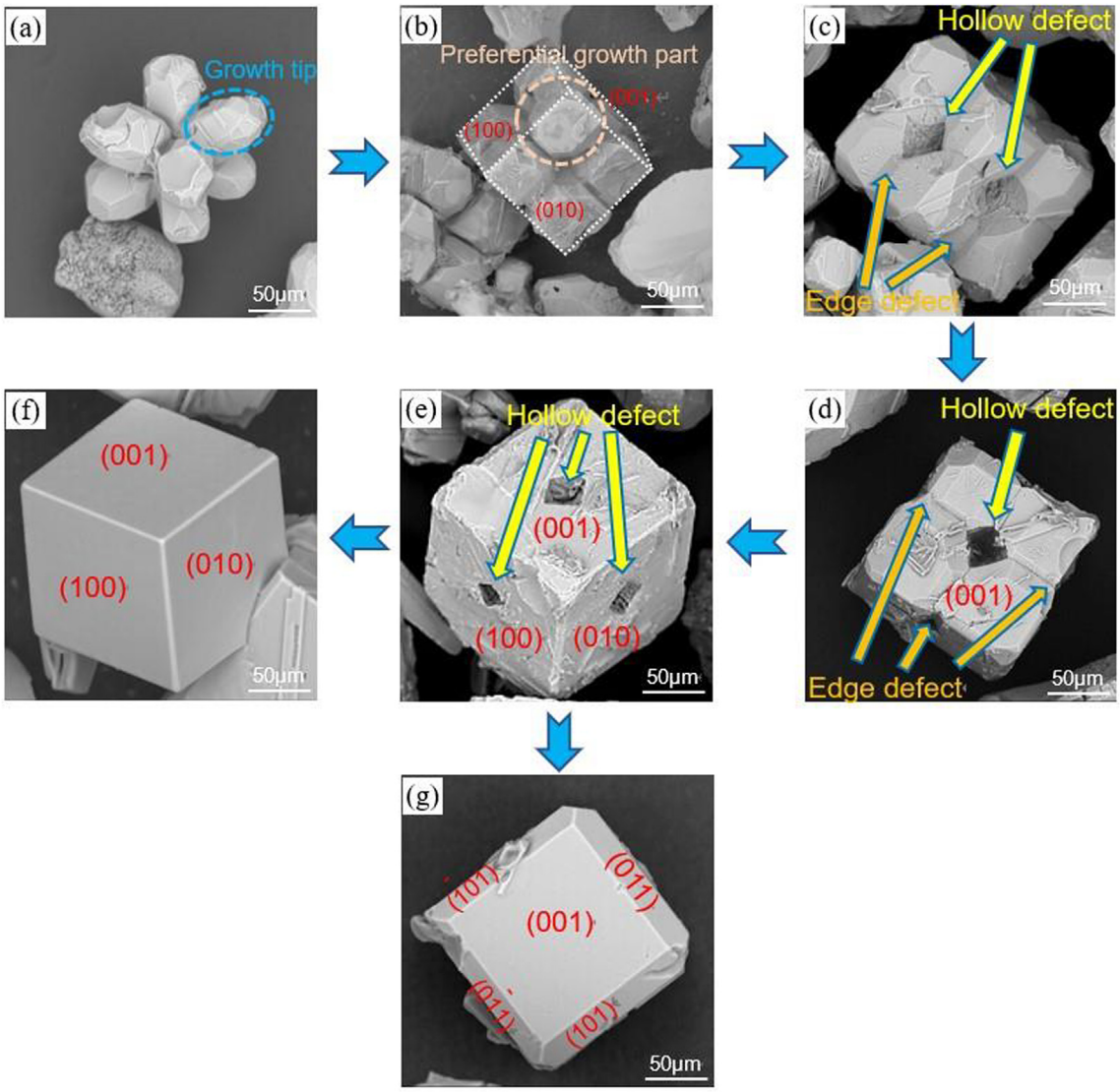

Fig. 3. Various morphologies of α-Al(FeMnCr)Si crystal at different growth stages and the evolution transition to the final cube.

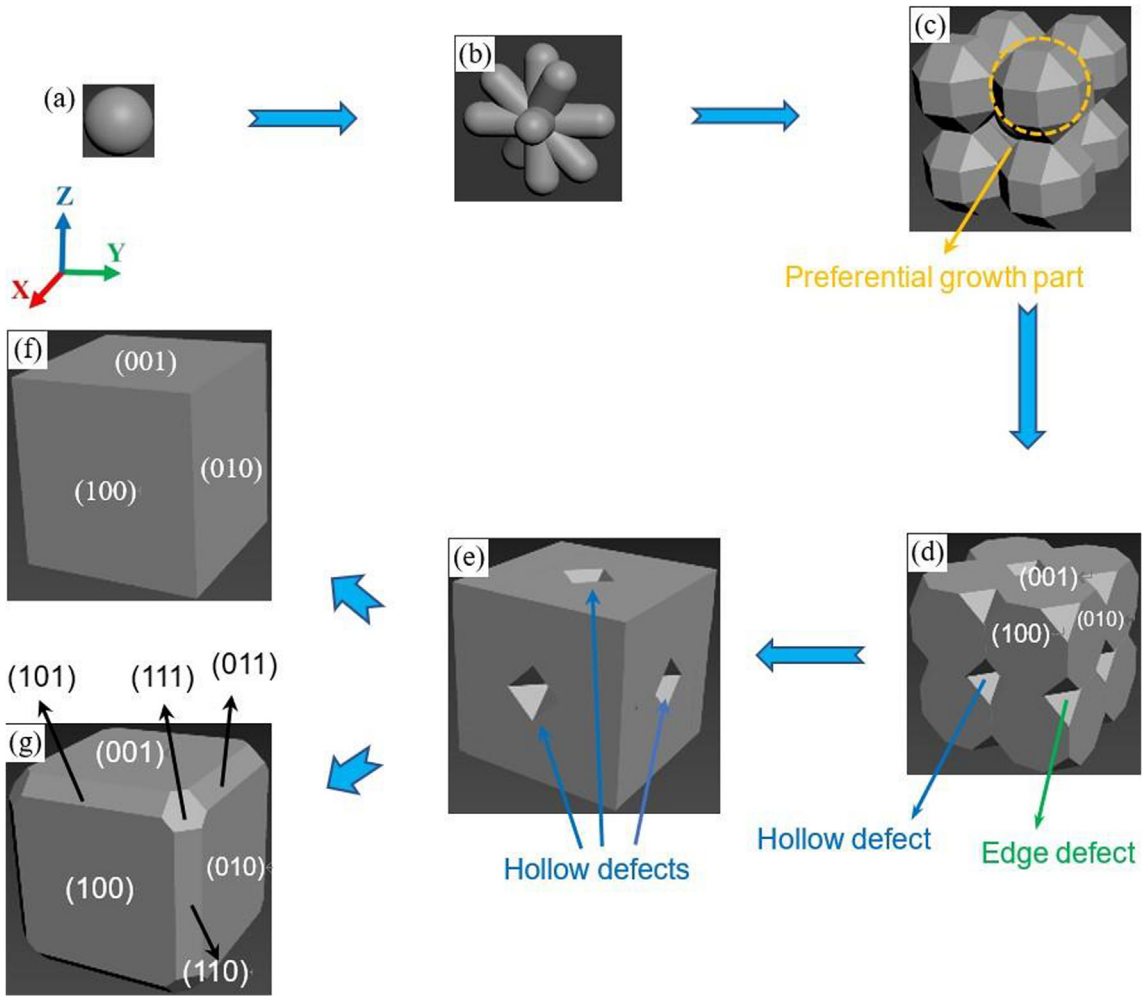

Fig. 4. Schematic growth process of the cubic α-Al(FeMnCr)Si crystal.

energy principle (Fig. 4(a)). Preferential growth along 8 vertical top angle directions is expected for the crystal, as shown in Fig. 4(b). This results in the formation of skeleton of a cubic crystal with 8 parts of small truncated polyhedron (Fig. 4(c) and Fig. 3(b)). These polyhedrons closely contact on their {100} faces, and the collection of some {111} faces on the corner of each polyhedron forms a hollow space in the middle of the large cube (Fig. 4(d)). With the continued growth, the defects of edges and {100} faces are filled by solute atoms in Fig. 4(e) and (f). In order to further decrease interface energy of crystal, the hollow defect gradually be filled at the final growth stage and a complete cubic crystal forms in Fig. 4(f). A truncated cube α-Al(FeMnCr)Si is also possible, because the filling of solute atoms on the edge of {100} faces is restrained, which may be caused by impurity concentrating on the edge. As shown in Figs. 3 and 4, preferential growth along 8 vertical top angle directions is a main feature which is different from lateral growth of β-AlFeSi and [111] edge growth of α-Al (FeMn)Si. Moreover, with appearance of {100} faces in growth process, it forms F faces (flat faces) of the crystal surface when supersaturation of 2D nucleation and growth is low enough. The faces in the defects of hollow and edge can be regarded as S and K faces (stepped and kinked faces), which provide more kinked locations for growth and high growth rate, as show in Fig. 4(c) and (d). These aspects result in that the complete cube α-Al (FeMnCr)Si crystal is the dominated morphology rather than defected-cube crystal.

4. Conclusion

In this paper, the morphology evolution and growth mechanism of primary α-Al(FeMnCr)Si were investigated. This intermetallic crystal exhibit cubic morphology at a low growth rate, which is covered by six {100} faces and shows preferential growth in eight points of the cube. A potential growth process of the cubic α-Al (FeMnCr)Si crystal is derived according to the observation of transition morphologies at different growth stages. Commonly, a crystal with a regular cubic morphology shows a low moving resistance in melt, which is convenient to the high-efficiency elimination by physical separation process. This work indicates that a low cooling rate combining with an appropriate holding time is necessary to form regular and cubic α-Al(FeMnCr)Si crystal in aluminum alloy melt. This is beneficial to the separation of Fe-containing intermetallic from melt, decreasing the Fe level and reducing its detrimental effect to the aluminum alloys.

CRediT authorship contribution statement

Dongtao Wang: Conceptualization, Investigation, Data curation, Writing - original draft. **Xiaozu Zhang:** Methodology, Writing - review & editing. **Hiromi Nagaumi:** Conceptualization, Funding acquisition, Resources, Supervision, Writing - review & editing, Project administration. **Xinzhong Li:** Methodology, Resources,

Writing - review & editing. **Haitao Zhang:** Supervision, Writing - review & editing.

Declaration of Competing Interest

The authors declare that they have no known competing financial interests or personal relationships that could have appeared to influence the work reported in this paper.

Acknowledgements

This project was supported by the China Postdoctoral Science Foundation (Grant No. 2019M661928) and National Natural Science Foundation of China (Grants Nos. U1864209 and 51771066).

References

[1] C.B. Basak, N.H. Babu, Mater. Des. 108 (2016) 277–288.
[2] L. Kucharikova, E. Tillová, M. Chalupová, M. Mazur, A. Herčko, R. Čička, Transp. Res. Procedia 40 (2019) 59–67.
[3] E. Tillová, M. Chalupová, L. Hurtalová, Evolution of phases in a recycled Al-Si cast alloy during solution treatment, Scanning Electron Microscopy, InTech (2012) 411–438.
[4] N.C.W. Kuijpers, F.J. Vermolen, K. Vuik, S.V.D. Zwaag, Mater. Trans. 44 (2003) 1448–1456.
[5] S. Terzi, J.A. Taylor, Y.H. Cho, L. Salvo, M. Suéry, E. Boller, A.K. Dahle, Acta Mater. 58 (2010) 5370–5380.
[6] T. Gao, Y. Wu, C. Li, X.F. Liu, Mater. Lett. 110 (2013) 191–194.
[7] H. Becker, A. Leineweber, Mater. Charact. 141 (2018) 406–411.
[8] B.G. Dietrich, H. Becker, M. Smolka, A. Kesler, A. Leineweber, G. Wolf, Adv. Eng. Mater. 19 (2017) 1700161.
[9] E. Tillová, M. Chalupová, L. Kucharikova, I. Švecová, J. Belan, Manuf. Technol. 19 (2019) 874–879.
[10] L. Ceschini, A. Morri, S. Toschi, L. Boromei, A. Bjurensted, S. Seifeddine, Metall. Ital. 108 (2016) 77–80.
[11] A. Bjurenstedt, D. Casari, S. Seifeddine, R.H. Mathiesen, A.K. Dahle, Acta Mater. 130 (2017) 1–9.
[12] D.F. Song, S.C. Wang, Y.L. Zhao, S.H. Liu, Y. Du, Y.H. Kang, Z. Wang, W.W. Zhang, Trans. Nonferrous Met. Soc. China 30 (2020) 1–13.
[13] L.T. Xiao, S. Da, X.Z. Ming, B.D. Sun, Y.H. Zhou, Trans. Nonferrous Met. Soc. China 1 (2001) 30–34.
[14] D.F. Chen, Z.Q. Cao, M. Yang, T. Zhang, Mater. Rev. 5 (2007) 341–348.
[15] Sunagawal. Crystals growth, morphology, perfection, Cambridge University Press, New York, 2005.